Carbohydrate Polymers 87 (2012) 2624–2629

Contents lists available at SciVerse ScienceDirect

Carbohydrate Polymers

journal homepage: www.elsevier.com/locate/carbpol

Plasticizing effect of 1-allyl-3-methylimidazolium chloride in cellulose acetate based polymer electrolytes

S. Ramesh [a,*], R. Shanti [a], Ezra Morris [b]

[a] Centre for Ionics University Malaya, Department of Physics, Faculty of Science, University of Malaya, 50603 Kuala Lumpur, Malaysia
[b] Faculty of Engineering and Science, Universiti Tunku Abdul Rahman, 53300 Kuala Lumpur, Malaysia

ARTICLE INFO

Article history:
Received 30 September 2011
Received in revised form
10 November 2011
Accepted 11 November 2011
Available online 22 November 2011

Keywords:
Ionic liquid
Complexation
Amorphous region
XRD analysis

ABSTRACT

1-Allyl-3-methylimidazolium chloride, [Amim] Cl was used to improve the stability and disrupt the crystallinity of the matrix formed between cellulose acetate (CA) and lithium bis(trifluoromethanesulfonyl)imide (LiTFSI) by solution casting technique. The sample composition of CA:LiTFSI:[Amim] Cl (14 wt.%:6 wt.%:80 wt.%) exhibits the highest ionic conductivity and has greater ability to retain minimum reduction value of 1.75×10^{-3} S cm^{-1} even after 30 days of storage at room temperature. Increase in [Amim] Cl doping induces greater structural disorderliness which is revealed by the XRD analysis. This is due to the complexation between the added constituents evident from the variation in FTIR spectra. The relaxation time of Li^+ ions is reduced due to the increase in amorphous region as observed by the shift of loss tangent peaks to higher frequencies and thus enhancing the ionic conductivity.

1. Introduction

Polymer electrolyte is a component that resides between the two differently charged electrodes in batteries. The presence of this thin membrane is crucial for transporting the mobile Li^+ ions between the electrodes in a safe manner to produce ionic conductivity. In order to permit the transportation of Li^+ conducting ions within the polymer electrolytes the existence of amorphous regions in the polymer matrix is vital. The above mentioned amorphous region provides an insight on the presence of coordinating sites that allows the mobility of Li^+ ions in between the polymer segments.

Previously amorphous polymer electrolytes were fabricated by employing various synthetic types of polymer. Ever since this invention started to impart an undeniable threat to the environment which taxes today's world, a number of solutions are being initiated to overcome this drawback. The main reason for these environmental hazard practices is the lack of systematic cost efficient disposal techniques (Norashikin & Ibrahim, 2009). In an effort to cope up with the above mentioned threat, this research was undertaken for developing biodegradable thin films using natural polymers. This development is believed to cover a wide scope of importance in the future due to their numerous applications in electronic devices such as fuel cells, solar cells, electrochromic windows and solar-state batteries (Armand, 1986; Rajendran, Sivakumar, & Subadevi, 2004; Ratner & Shriver, 1988; Shriver et al., 1981; Siva Kumar, Subrahmanyam, Jaipal Reddy, & Subba Rao, 2006).

The natural polymer that gains interest in this present work is cellulose acetate (CA). The widespread use of CA is attributed to the availability of renewable resources, non-toxic nature, low cost and also due to its biodegradable nature (Averous, Fringant, & Moro, 2001; Wu, Wang, Li, Li, & Wang, 2009). It is well established that Li^+ ion coordination takes place predominantly in the amorphous domain but since natural polymers are highly crystalline therefore CA alone cannot be a suitable medium for the production of polymer electrolytes.

To resolve this barrier, a type of ionic salt, LiTFSI was embedded in the CA matrix. The LiTFSI gains interest owing to its large electronegativity, low lattice energy and delocalization of charge (Ramesh & Lu, 2008). These properties promote high degree of dissociation of LiTFSI in the CA matrix and allow the free ions to remain in its ionic state to continuously participate in ion conduction. The incorporation of LiTFSI induces structural disorderliness but the extent of enhancement in the ionic conductivity is not sufficiently high to be used in electronic devices. This was attributed to the large anionic size ($TFSI^-$) which has a low tendency to break the strong bonding network between the atoms that are connected to the polar functional group in CA and thus lowering the number of vacant sites that will be available for lithium ion (Li^+)

* Corresponding author. Tel.: +60 3 79674391.
E-mail addresses: rameshtsubra@gmail.com (S. Ramesh), shanthy87@yahoo.com (R. Shanti), ezram@utar.edu.my (E. Morris).

0144-8617/$ – see front matter © 2011 Elsevier Ltd. All rights reserved.
doi:10.1016/j.carbpol.2011.11.037

Table 1
Compositions and relaxation frequencies of the designated CA:LiTFSI:[Amim] Cl polymer electrolytes.

Designation	Composition of CA:LiTFSI:[Amim] Cl (wt.%)	Relaxation frequency, $\log \omega_m$ (Hz)
IL-0	70:30:0	5.60
IL-40	49:21:40	5.80
IL-80	14:6:80	6.50

coordination. Herewith, the crystallinity in CA:LiTFSI matrix was further suppressed by plasticizing with [Amim] Cl.

The incorporation of [Amim] Cl in polymer electrolytes was an innovative approach to develop high conducting CA based polymer electrolytes due to their high mobility and high concentration of carrier ions (Ning, Xingxiang, Haihui, & Benqiao, 2009). Despite this, [Amim] Cl does posses an unusual solvent property in dissociating the crystalline polymers (Cuissinat, Navard, & Heinze, 2008). This unusual solvent property was attributed to high chloride ion concentration and a specific activity of [Amim] Cl which breaks the extensive hydrogen bonding network and allows the polar oxygen atom in the polymer to form coordination with the free mobile ions (Swatloski, Spear, Holbrey, & Rogers, 2002). Some other listed properties of [Amim] Cl are non-volatility, non-flammability, low viscosity and chemical and electrochemical stability (Kubisa, 2004; Ning et al., 2009; Sing & Sekhon, 2005; Welton, 1999).

The efficiency of the developed biodegradable polymer electrolytes with different plasticization ratio of [Amim] Cl will be discussed in this communication. This was rationalized in terms of the ionic conductivity, complexation, phase identification and relaxation time of the Li^+ mobile ions.

2. Experimental

2.1. Materials

Material		Supplier[a]
Name	Abbreviation	
Cellulose acetate (M_w = 61,000 g mol^{-1})	CA	A
Lithium bis(trifluoromethanesulfonyl)imide	LiTFSI	F
1-Allyl-3-methylimidazolium chloride	[Amim] Cl	A
N,N-dimethylformamide	DMF	R & M

[a] *Note*: A, Aldrich; F, Fluka; R & M, R & M Chemicals.

2.1.1. Preparation of thin film

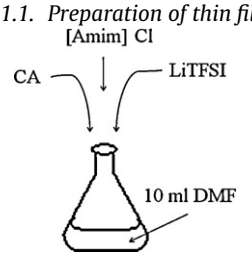

2.2. Characterizing technique

2.2.1. Impedance spectroscopy

The thickness of the thin film was measured with a micrometer screw gauge before subjecting to ionic conductivity measurement using a HIOKI Model 3532-50 Hi-Tester. The measurements were taken over the frequency ranging from 50 Hz to 5 MHz with the thin film sandwiched in between two stainless steel blocking electrodes having an area of 4.9807 cm^2. The obtained impedance plot was used to find the bulk resistance (R_b) value for calculating the exerted ionic conductivity by substituting in the equation:

$$\sigma = \frac{L}{R_b A} \quad (1)$$

where σ is the conductivity in S cm^{-1}, L refers to the thickness of thin film in cm, R_b is the bulk resistance in Ω and A represents the surface area of the stainless-steel blocking electrodes in cm^2. The ionic conductivity of thin films was monitored over the storage time of 30 days with every 10 days of interval. The dissipation factor graph of tan δ against log ω was plotted using the following equations:

$$\tan \delta = \frac{\varepsilon''}{\varepsilon'} \quad (2)$$

where tan δ represents the loss tangent whereas ε' and ε" signify the real and imaginary portion of permittivity, respectively.

$$\log \omega = \log(2\pi f) \quad (3)$$

where ω represents the angular frequency and f refers to frequency.

The values of ε', ε" and f were obtained from the impedance plot of freshly casted samples at ambient temperature.

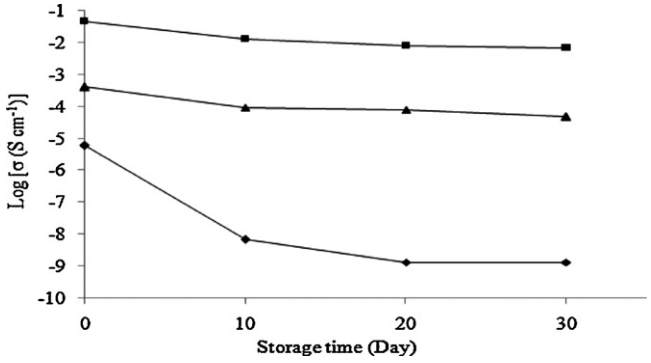

Fig. 1. Variation of log ionic conductivity at room temperature with storage time for samples IL-0 (♦), IL-40 (▲) and IL-80 (■).

2.2.2. Fourier transform infrared (FTIR)-horizontal attenuated total reflection (HATR) analysis

Perkin-Elmer FTIR Spectrometer, Spectrum RX1, and a HATR compartment were used to determine the occurrence of complexation between the constituents. All the readings were recorded in the wave region between 4000 and 600 cm^{-1} with the resolution of 4 cm^{-1}. The FTIR spectra were recorded in the transmittance mode.

2.2.3. XRD analysis

The X-Ray Diffraction (XRD) analysis was performed on selected samples with the aid of Siemens D-5000 Diffraction System using Cu-K_α radiation having the wavelength of 1.5406 Å. The respective XRD pattern was recorded for the Bragg angles (2θ) ranging from 5° to 80° at room temperature.

3. Results and discussion

3.1. Ionic conductivity studies

The variation of ionic conductivity of polymer electrolytes with different [Amim] Cl containing was tested over the storage time of 30 days and the results are as presented in Fig. 1.

3.1.1. Effect of manipulating [Amim] Cl content

The placement of the ionic conductivity plots varies with [Amim] Cl content. The sample IL-80 is displayed at the highest

range followed by sample IL-40 and finally IL-0. This reveals that the ionic conductivity of polymer electrolytes improves with increase in [Amim] Cl content. The underlying principle for the enhancement in ionic conductivity is attributed to the increase in the concentration of amorphous phase upon the disruption of bonding between the oxygen (O) and acetate (Ac) atom in –OAc functional group in CA. This allows greater availability of vacant oxygen to assist the lithium ions (Li^+) mobility by forming temporary ionic interaction. This interaction aids the continuous hopping of Li^+ ions from one vacant site to another with ease and thus enhances the ionic conductivity (Uma, Mahalingam, & Stimming, 2003).

The addition of high self-dissociating [Amim] Cl (Jiang, Gao, Li, & Su, 2006) promotes the dissociation of LiTFSI in CA matrix by weakening the inter-ion Coulombic force that holds the two differently charged ions, forming free ions (Li^+ and $TFSI^-$). Thus, increasing plasticization of [Amim] Cl increases the number of free mobile Li^+ ions that participate in ion conduction which is another contributing factor for the observed ionic conductivity enhancement in Fig. 1. The anion, $TFSI^-$ induces structural disorderliness in CA matrix.

The ionic conductivity enhancement can be further justified by the increase in the number of transit site (Cl^-) obtained upon the dissolution of [Amim] Cl particles in the CA matrix. This transit site provides an alternative pathway for the mobility of Li^+ ions present in the surroundings when the neighboring oxygen atom is in the coordination state with another Li^+ ion (Yahya et al., 2006). Hence, the mobility of free Li^+ ions is assured and more frequent ionic transfer is expected to occur thus enhancing the ionic conductivity.

3.1.2. Effect of storage time on the ionic conductivity

This study is focused on investigating the influence of [Amim] Cl content on the aging effect of the CA:LiTFSI:[Amim] Cl system. In order to accomplish this, the ionic conductivity of samples IL-0, IL-40 and IL-80 were monitored for the storage time of 30 days at room temperature. In general, addition of [Amim] Cl improves the aging effect in immense proportion.

With reference to Fig. 1, it can be understood that the sample IL-0 experience greater aging effect evident through an enormous decline in the ionic conductivity compared to the [Amim] Cl plasticized samples, IL-40 and IL-80. This reveals that IL-0 does not have the ability to retain ionic conductivity for a longer storage time ascribed to its high crystallinity which has low liquid retention ability. Thus, more liquid component will be dissipated from the matrix over time and induces the continuous drop in ionic conductivity.

Incorporation of increasing [Amim] Cl content in the polymer electrolytes gradually improves the ability to retain the ionic conductivity over the entire storage time, making it more aging resistant. This is due to the greater disruption in the matrix crytallinity that increases the amorphous fraction which induces more availability of polar functional groups that have high liquid retention capability (Ramesh & Arof, 2009). The dissociation of [Amim] Cl in the matrix also provides additional polar groups for the purpose of retaining the liquid components. Therefore, more traces of liquid component will be trapped between the CA matrix providing a dilute medium to ease the Li^+ ions motion and hence retain the ionic conductivity over the storage time (Ramesh & Arof, 2009).

On the other hand, it can also be found that all the tested polymer electrolytes do not exhibit any dramatic change in ionic conductivity after 10 days. This proves that the samples retain high chemical integrity overcoming the solvent leakage limitation over storage time. These results show that the increase in [Amim] Cl content in CA:LiTFSI:[Amim] Cl matrix improves the stability of polymer electrolytes by retaining their integrity over the storage time.

Table 2
Band assignments and wavenumbers exhibited by pure constituents.

Sample	Band assignments	Wavenumber (cm^{-1})
CA	O–H stretching	3445
	C–H stretching (CH_3)	2932
	C–H stretching (CH_2)	2879
	C=O symmetric	1734
	C=O asymmetric	1656
	CH_2 bending	1436
	C–H bending	1369
	C–O–C asymmetric bridge stretching	1158
	C–O–C stretching of the pyrose ring	1032
	δ C–H	901
LiTFSI	O–H	3419
	$S–CH_3$	2979 and 2876
	$C–SO_2–N$	1356
	$–CF_3$	1193
	C–F stretch	1142
	S=O	1065
[Amim] Cl	H_20 in materials	3369
	Alkyl C–H stretching	2962, 2941 and 2873
	0-H bending	1645
	Imidazole ring stretching	1573
	Imidazole H–C–C and H–C–N bending	1168
	In-plane Imidazole ring bending	849
	Out-of-plane C–H bending of imidazole ring	764

3.2. FTIR-HATR studies

FTIR spectroscopy is a well recognized fingerprinting technique used in perceiving the occurrence of complexation between the constituents present in both crystalline and amorphous phase. The complexation between the constituents were deduced by relying on the changes in the cage peak in terms of the frequency shifting, relative intensity, shape, disappearance of existing peak and even through the formation of new peaks. The FTIR spectra of polymer electrolytes vary according to their compositions and it is independent of concentration.

The band assignments for pure substances are summarized in Table 2 (da Conceiçao, Lucena, de Alencar, Mazzeto, & de Soares, 2003; Ramesh & Lu, 2008; Ranga Rao, Rajkumar, & B, 2009). The occurrence of complexation between pure CA and pure LiTFSI was confirmed based on the alternations in IL-0 spectrum as portrayed in Fig. 2. The first evidence of complexation was based on the characteristic peak of C=O symmetric present at 1734 cm^{-1} in pure CA which shifted to lower frequency at 1726 cm^{-1} in IL-0 after complexation with LiTFSI. The shifting of this characteristic peak proves the occurrence of complexation at this frequency range between the Li^+ ions and oxygen atoms in polymer backbone. The relative intensity of the interacting band was found to reduce from 64% (pure CA) to 55% (IL-0) upon complexation as represented in Fig. 3.

The occurrence of complexation between CA and LiTFSI was further verified by the band broadening effect at the frequency range of 1030–1250 cm^{-1} which results from the simple peak overlapping. The disappearance of peak at 1320 cm^{-1} in pure CA upon addition of LiTFSI reveals the detachment of acetate (–Ac) from the –OAc functional group via occurrence of complexation. A simple peak overlapping between a single intense peak at 1369 cm^{-1} in Fig. 2(a) with two peaks at 1356 and 1333 cm^{-1} in Fig. 2(b) results in a three peaks formation at 1367, 1348 and 1325 cm^{-1} in Fig. 2(c). The observed change in the shape of peak was one of the evidence to prove the complexation. The initial relative intensity of the peak that co-exists at 1656 cm^{-1} in pure CA was 61% and upon complexation with LiTFSI this peak was displaced to higher frequency at

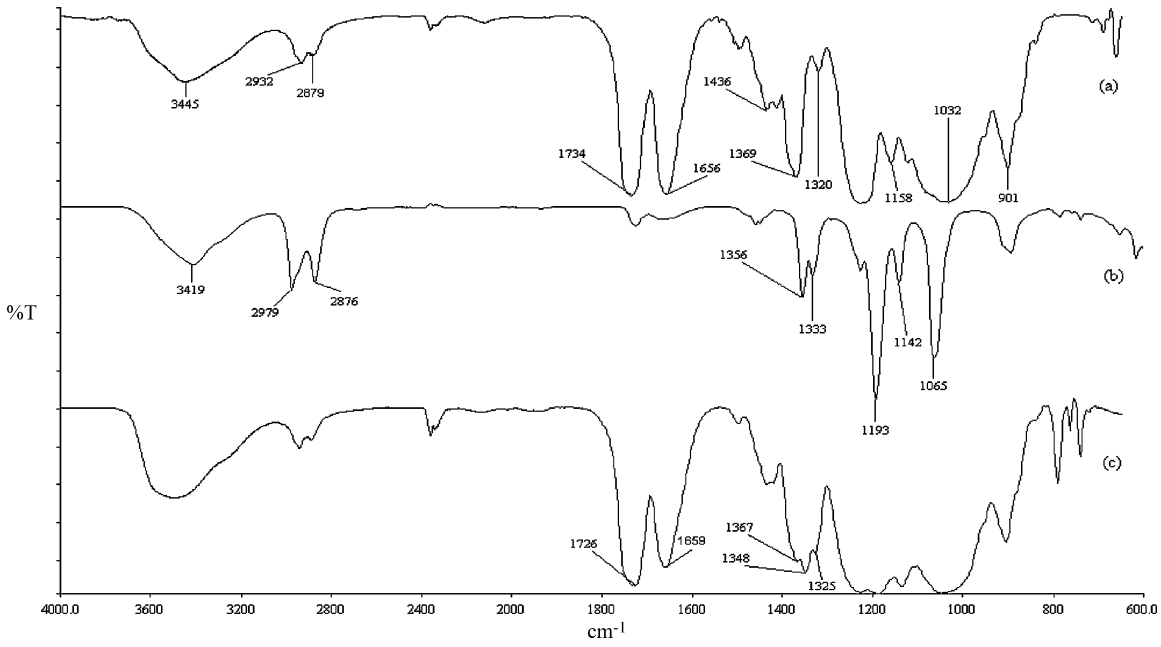

Fig. 2. FTIR spectra of (a) pure CA, (b) pure LiTFSI and (c) IL-0.

1659 cm^{-1} with reduced relative intensity (47%) in IL-0. The shifting to higher frequency proves the weaker interaction between Li^+ ions and oxygen atom in C=O asymmetric.

The same technique was relied to deduce the possible complexation between different content of [Amim] Cl in CA:LiTFSI:[Amim] Cl matrix. The dominant interest to find out the possible complexation was gained by sample IL-40 and IL-80 whereby the respective spectra are presented in Fig. 4 together with IL-0 and pure [Amim] Cl. The first evidence to prove the complexation was based on the displacement of C=O characteristic peak initially present at 1726 cm^{-1} in Fig. 4(a) and 1732 cm^{-1} in Fig. 4(b). The C=O peak was shifted to higher frequency at 1745 cm^{-1} in Fig. 4(c) upon complexation and further addition of [Amim] Cl induce the displacement at lower frequency in Fig. 4(d) with the value of 1742 cm^{-1}. The observed reduction in frequency with further addition of [Amim] Cl suggests greater interaction between increasing amount of Li^+ ions and oxygen atom. Apart from this, the respective peak also experienced an increase in the relative intensity with further addition of [Amim] Cl with the calculated value from 54% in IL-40 to 70% in IL-80. The increase in the relative intensity proves the increase in number of Li^+ ions that form complexation with the oxygen atom at this frequency, upon increase in [Amim] Cl content that effectively overcomes the inter-Coulombic force between the differently charged ions in LiTFSI making more availability of Li^+ ions.

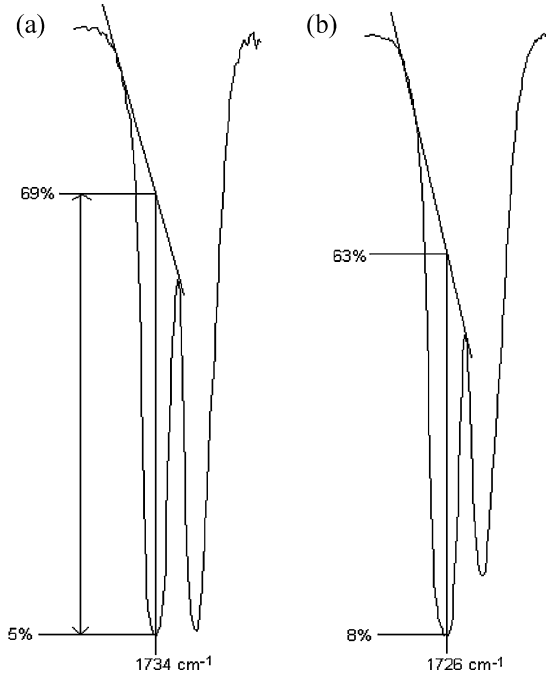

Fig. 3. The changes in intensity of C=O symmetric band for (a) pure CA and (b) IL-0.

Other evidence to prove the complexation was focused on the peak at 1573 cm^{-1} in pure [Amim] Cl. This intense peak was changed to a small peak (1575 cm^{-1}) as in IL-40 upon the complexation with CA and LiTFSI and further addition of [Amim] Cl in the polymer electrolytes induce to an increase in the relative intensity as in IL-80 (1571 cm^{-1}). The small peak that co-exist at 1497 cm^{-1} in IL-0 becomes more intense without no change in its frequency upon the complexation with [Amim] Cl and consequently absent at highest [Amim] Cl containing sample, IL-80.

A simple overlapping between the peak at 1659 cm^{-1} and 1645 cm^{-1}, respectively in IL-0 and pure [Amim] Cl is able to deduce the complexation. The result of this overlapping is the presence of broader peak both in IL-40 and IL-80, respectively at 1654 and 1638 cm^{-1}. The broad peak at 1654 cm^{-1} in IL-40 was shifted to lower wavelength at 1638 cm^{-1} in IL-80, showing greater extent of interaction between the Li^+ ions and oxygen atom. This reference peak was found to decline in broadness as more [Amim] Cl is incorporated which would attribute to the decrease in the number of Li^+ ions that forms complexation with the oxygen atoms at this frequency. This was attributed to the vast presence of nitrogen atoms in [Amim] Cl which have higher tendency to form coordination with Li^+ ions than the oxygen owing to its better electron donating feature.

3.3. X-ray diffraction studies

X-ray diffraction measurements were performed on polymer electrolytes plasticized with different [Amim] Cl content to deduce the degree of amorphocity at room temperature. The diffraction

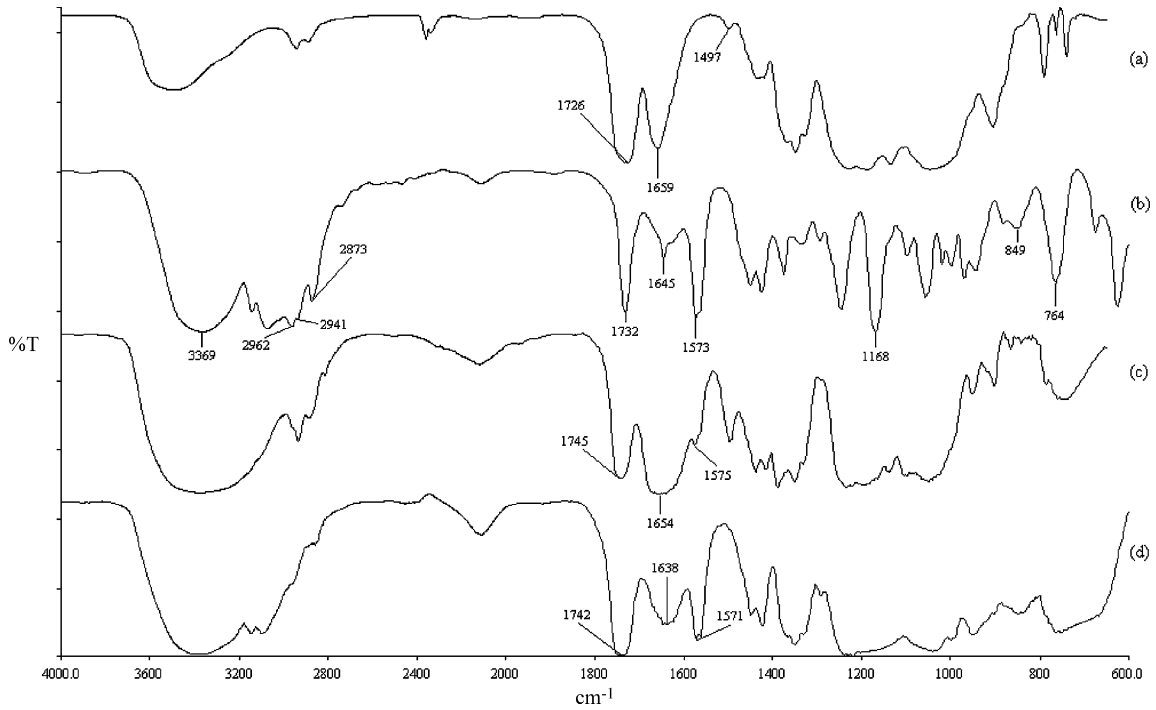

Fig. 4. FTIR spectra of (a) IL-0, (b) pure [Amim] Cl, (c) IL-40 and (d) IL-80.

patterns of pure CA (thin film), pure LiTFSI, IL-0, IL-40 and IL-80 are represented in Fig. 5.

In view of the inset graph in Fig. 5, the appearance of a single intense diffraction peak centered at $2\theta = 13.5^\circ$ shows the typical characteristic of a crystalline microstructure of pure LiTFSI. This intense peak was found to be absent in sample IL-0 associated to the complete dissolution of the LiTFSI in CA matrix which further suppresses the crystalline phase. This was validated through the disappearance of the moderate intense peak at $2\theta = 8.5^\circ$, 10.5° and 13.5° in pure CA and accompanied by a substantial broadening in the IL-0 diffraction peak. Additionally, the peaks that remained undisturbed upon addition of LiTFSI at $2\theta = 17.5^\circ$ and 23.5° in IL-0 were found to disrupt and a substantial broadening in the diffraction peak occurs at the angle range between 5° and 30° with increase in [Amim] Cl content.

It also been observed that the diffraction peak substantially increased in broadness and decreased in intensity with increase in [Amim] Cl content in the polymer electrolytes. This observation indicates the considerable decrease in the degree of crystallinity of CA matrix as more [Amim] Cl particles are being incorporated in the polymer electrolytes. The associated reduction in crystallinity was caused by the significant structural reorganization imposed by [Amim] Cl that induces greater structural disorderliness. Hence, increase in amorphous region causes increase in the number of transit sites which improves the ionic transport and induces greater ionic conductivity (Baskaran, Selvasekarapandian, Kuwata, Kawamura, & Hattori, 2006).

With reference to the results, it can be clarified that greater structural conversion occurs predominantly at the highest [Amim] Cl containing sample, IL-80, allowing it to be present in highly amorphous morphology permitting greater Li^+ ion transportation. Thus, this polymer electrolyte composition appears as the highest conducting sample.

3.4. Frequency dependence of loss tangent study

This study was performed in order to understand the Li^+ ions transport mechanism when different content of [Amim] Cl was incorporated in CA:LiTFSI:[Amim] Cl matrix. Fig. 6 represents the plot of tan δ versus log ω for samples IL-0, IL-40 and IL-80.

By observing the plot, it was found that the appearance of peak in both the non-plasticized and plasticized samples discloses the

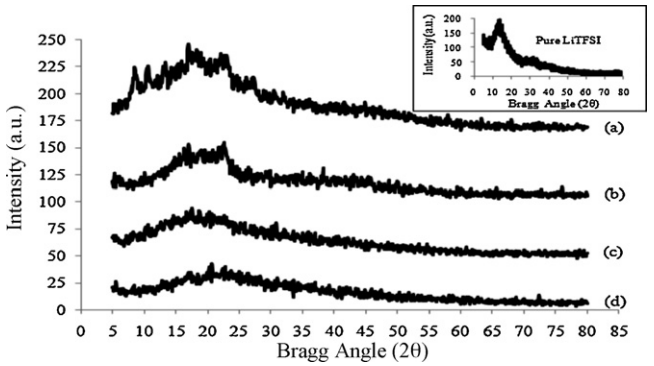

Fig. 5. The diffraction patterns of (a) pure CA (thin film), (b) IL-0, (c) IL-40, (d) IL-80 and pure LiTFSI in the inset.

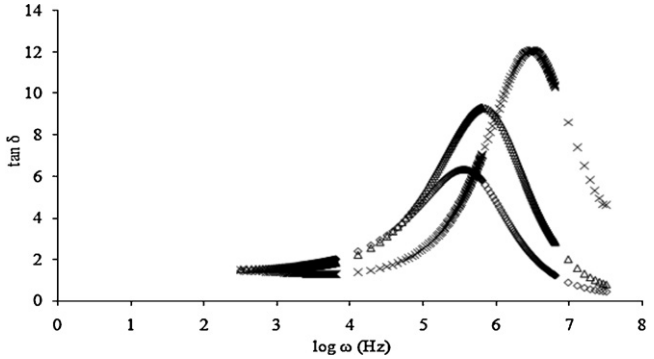

Fig. 6. Variation of tan δ of CA:LiTFSI thin films with frequency for IL-0 (◊), IL-40 (△) and IL-80 (x) at room temperature.

presence of relaxation dipoles in Li^+ ions in all the tested samples (Paradhan, Choundhary, & Samantaray, 2008). This confirms that mobility of Li^+ ions still persist upon addition of [Amim] Cl in the matrix.

This plot also provides an insight on the Li^+ ions mobility upon the presence of different [Amim] Cl content. It can be visualized from the relaxation frequency ($\log_{max}\omega$) values tabulated in Table 1, the loss tangent peaks shifted continuously towards higher frequencies upon the increase in the [Amim] Cl content. This shifting phenomenon illustrates the reduction in the relaxation time of Li^+ ions, which speeds up the mobility as more amorphous elastomeric region becomes available with increase in [Amim] Cl content in the polymer electrolytes matrix (Paradhan et al., 2008).

The increase in the number of non-bridging ions in [Amim] Cl (Cl^-) increases the Li^+ ions transfer capacity. The non-bridging ions act as an additional transit site that permits the mobility of Li^+ ions along the polymer backbone. The presence of the transit site shortens the distance for the Li^+ ions to hop from one unoccupied oxygen to another in polymer chain, acquiring less energy loss for the mobility of ion. Hence, frequent migrations of mobile ions are expected to occur that is crucial in enhancing the ionic conductivity.

The influence of different addition of [Amim] Cl content on the number of Li^+ ions that participate in ion conduction can be determined based on the magnitude of the $\tan\delta$ (Azizi Samir, Alloin, Sanchez, Gorecki, & Dufresne, 2004). The magnitude of the $\tan\delta$ increases upon increase in [Amim] Cl content which indicates the increase in the number of Li^+ ions that participates in the relaxation process to assist the ionic conductivity as indicated by the area under the loss factor peak. The increase in Li^+ ions concentration proves the efficiency of [Amim] Cl in overcoming the inter-coulombic force in LiTFSI, making more Li^+ ions to be available for enhancing the ionic conductivity.

As the content of [Amim] Cl in polymer electrolytes is increased, more numbers of transit sites (Cl^-) are available, creating an alternative pathway that is beneficial for easing the Li^+ ion transport which is crucial in achieving high ionic conductivity. The highest ionic conductivity was achieved by sample IL-80 having high concentration of amorphous phase coupled with greater presence of Li^+ ions.

4. Conclusion

Hydrophilic [Amim] Cl containing high chloride ion concentration has strong hydrogen bond-forming abilities with CA which is capable of plasticizing the CA:LiTFSI matrix and induces an enhancement in the ionic conductivity while retaining the integrity over the storage time. IL-80 is the highest conducting sample which has the greatest ability to retain ionic conductivity even after 30 days of storage time with the value of 1.75×10^{-3} S cm^{-1} at room temperature owing to the high concentration of polar functional groups that have good liquid retention capability. The shift of loss tangent peaks towards higher frequencies with increase in [Amim] Cl content suggests the increase in Li^+ ions' mobility has improved in the amorphous fraction. Therefore, the ionic conductivity enhances with the increase in [Amim] Cl content. The structural alternations upon the complexations of chemical constituents were confirmed by XRD and FTIR analysis.

Acknowledgements

This work was supported by the Fundamental Research Grant Scheme (FRGS) from Ministry of Higher Education, Malaysia (FP009/2010B) and Universiti Malaya Research Grant (UMRG: RG140-11AFR).

References

Armand, M. B. (1986). Polymer electrolytes. *Annual Review of Materials Science*, *16*, 245–261.
Averous, L., Fringant, C., & Moro, L. (2001). Plasticized starch–cellulose interactions in polysaccharide composites. *Polymer*, *42*, 6565–6572.
Azizi Samir, M. A. S., Alloin, F., Sanchez, J.-Y., Gorecki, W., & Dufresne, A. (2004). Nanocomposite polymer electrolytes based on poly(oxyethylene) and cellulose nanocrystals. *The Journal of Physical Chemistry B*, *108*, 10845–10852.
Baskaran, R., Selvasekarapandian, S., Kuwata, N., Kawamura, J., & Hattori, T. (2006). Conductivity and thermal studies of blend polymer electrolytes based on PVAc-PMMA. *Solid State Ionics*, *177*, 2679–2682.
Cuissinat, C., Navard, P., & Heinze, T. (2008). Swelling and dissolution of cellulose. Part IV: Free floating cotton and wood fibres in ionic liquids. *Carbohydrate Polymer*, *72*, 590–596.
da Conceiçao, M., Lucena, C., de Alencar, A. E. V., Mazzeto, S. E., & de Soares, S. (2003). The effect of additives on the thermal degradation of cellulose acetate. *Polymer Degradation Stability*, *80*, 149–155.
Jiang, J., Gao, D., Li, Z., & Su, G. (2006). Gel polymer electrolytes prepared by in situ polymerization of vinyl monomers in room-temperature ionic liquids. *Reactive & Functional Polymers*, *66*, 1141–1148.
Kubisa, P. (2004). Application of ionic liquids as solvents for polymerization processes. *Progress in Polymer Science*, *29*, 3–12.
Ning, W., Xingxiang, Z., Haihui, L., & Benqiao, H. (2009). 1-Allyl-3-methylimidazolium chloride plasticized-corn starch as solid biopolymer electrolytes. *Carbohydrate Polymers*, *76*, 482–484.
Norashikin, M. Z., & Ibrahim, M. Z. (2009). The potential of natural waste (corn husk) for production of environmental friendly biodegradable film for seedling. *World Academy of Science, Engineering and Technology*, *58*, 176–180.
Paradhan, D. K., Choundhary, R. N. P., & Samantaray, B. K. (2008). Studies of dielectric relaxation and AC conductivity behavior of plasticized polymer nanocomposite electrolytes. *International Journal of Electrochemical Science*, *3*, 597–608.
Rajendran, S., Sivakumar, M., & Subadevi, R. (2004). Investigations on the effect of various plasticizers in PVA-PMMA solid polymer blend electrolytes. *Materials Letters*, *58*, 641–649.
Ramesh, S., & Lu, S.-C. (2008). Effect of nanosized silica in poly (methyl methacrylate)-lithium bis(trifluoromethanesulfonyl)imide based polymer electrolytes. *Journal of Power Sources*, *185*, 1439–1443.
Ramesh, S., & Arof, A. K. (2009). A study incorporating nano-sized silica into PVC-blend-based polymer electrolytes for lithium batteries. *Journal of Materials Science*, *44*, 6404–6407.
Ranga Rao, G., Rajkumar, T., & Babu, Varghese. (2009). Synthesis and characterization of 1-butyl 3-methylimidazolium phosphomolybdate molecular salt. *Solid State Sciences*, *11*, 36–42.
Ratner, M. A., & Shriver, D. F. (1988). Ion transport in solvent-free polymers. *Chemical Reviews*, *88*, 109–124.
Shriver, D. F., Papke, B. L., Ratner, M. A., Dupon, R., Wong, T., & Brodwin, M. (1981). Structure and ion transport in polymer–salt complexes. *Solid State Ionics*, *5*, 83–88.
Sing, B., & Sekhon, S. S. (2005). Ion conducting behaviour of polymer electrolytes containing ionic liquids. *Chemical Physics Letters*, *414*, 34–39.
Siva Kumar, J., Subrahmanyam, A. R., Jaipal Reddy, M., & Subba Rao, U. V. (2006). Preparation and study of properties of polymer electrolyte system (PEO + $NaClO_3$). *Materials Letters*, *60*, 3346–3349.
Swatloski, R. P., Spear, S. K., Holbrey, J. D., & Rogers, R. D. (2002). Dissolution of cellulose with ionic liquids. *Journal of American Chemical Society*, *124*, 4974–4975.
Uma, T., Mahalingam, T., & Stimming, U. (2003). Mixed phase solid polymer electrolytes based on poly (methylmethacrylate). *Materials Chemistry and Physics*, *82*, 478–483.
Welton, T. (1999). Room-temperature ionic liquids. Solvents for synthesis and catalysis. *Chemical Reviews*, *99*, 2071–2083.
Wu, R.-L., Wang, X.-L., Li, F., Li, H.-Z., & Wang, Y.-Z. (2009). Green composite films prepared from cellulose, starch and lignin in room-temperature ionic liquid. *Bioresource Technology*, *100*, 2569–2574.
Yahya, M. Z. A., Ali, A. M. M., Mohammat, M. F., Hanafiah, M. A. K. M., Mustaffa, M., Ibrahim, S. C., et al. (2006). Ionic conduction model in salted chitosan membranes plasticized with fatty acid. *Journal of Applied Sciences*, *6*, 1287–1291.